Available online at www.sciencedirect.com
SCIENCE DIRECT®
Journal of Catalysis 220 (2003) 433–441
JOURNAL OF CATALYSIS
www.elsevier.com/locate/jcat

Support effect in hydrotreating catalysts: hydrogenation properties of molybdenum sulfide supported on β-zeolites of various acidities

Claude-Emmanuel Hédoire,[a] Catherine Louis,[a] Anne Davidson,[a] Michèle Breysse,[a,*] Françoise Maugé,[b] and Michel Vrinat [c]

[a] *Laboratoire de Réactivité de Surface, UMR CNRS 7609, Université Pierre et Marie Curie, 4 place Jussieu, 75252 Paris cédex, France*
[b] *Laboratoire de Catalyse et Spectrochimie, UMR CNRS 6506, ENSICaen, 6 boulevard du Maréchal Juin, 14050 Caen cédex, France*
[c] *Institut de Recherches sur la Catalyse, UPR CNRS 5401, 2 boulevard Albert Einstein, 69626 Villeurbanne cédex, France*

Received 26 March 2003; revised 26 June 2003; accepted 11 July 2003

Abstract

In order to better understand the role of the acidity of the support on the hydrogenation properties of a molybdenum sulfide phase, a β-zeolite with a nominal Si/Al = 13.8 was partially (Si/Al = 15.0 and 18.7) and fully dealuminated (Si/Al $\geqslant$ 800, no Brönsted acidity). To achieve a reasonable Mo loading with a high Mo dispersion, the Mo/β catalysts were prepared by cation exchange with $[Mo_3S_4(H_2O)_9]^{4+}$ in the presence of NH_3, followed by a thermal treatment under Ar at 623 K. This preparation method allowed us to introduce up to 4.7 wt% of Mo into the acidic zeolites. For the fully dealuminated zeolite that contains no exchange sites, Mo was introduced by impregnation with an aqueous solution of ammonium heptamolybdate. After sulfidation of all the samples in a stream of H_2/H_2S, MoS_2 slabs were observed by TEM. The electronic properties of the molybdenum sulfide phase were examined by means of IR spectroscopy of CO adsorption at 100 K. The ν(CO) wavenumber regularly increases with the acidity of the zeolite support from 2122 cm^{-1} for the nonacidic sample to 2158 cm^{-1} for the most acidic one. The hydrogenation activities of these catalysts determined in tetralin hydrogenation, and carried out in the presence of H_2S, also varied within a wide range, the most acidic catalyst being circa 40 times more active than the nonacidic one. This enhancement of activity in hydrogenation is related to the electron-deficient character of the sulfide particles in acidic zeolites.

Keywords: Molybdenum sulfide; β-Zeolite; Hydrogenation catalysts; Tetralin hydrogenation; Hydrotreatment; CO adsorption

1. Introduction

The great environmental significance of the hydrotreating process has led to a vivid research on the properties of sulfide catalysts [1,2]. The conventional hydrotreating catalyst is a Co (or Ni)-promoted MoS_2 (or WS_2) active phase supported on γ alumina. With the objective to improve the catalytic properties for the various reactions, hydrodesulfurization, hydrodenitrogenation, and aromatics hydrogenation, involved in the general term hydrotreatment, many attempts have been made to replace alumina by other supports [3]. The interest in dispersing the active phase in zeolites is multiple. Besides the large surface area of this support, which may allow the preparation of highly dispersed phases, the zeolite acidity can be utilized directly in bifunctional hydrocracking reactions or indirectly by transforming the most difficult compounds to desulfurize, i.e., 4,6-alkyldibenzothiophenes into more reactive compounds either through demethylation or through isomerization [2–4]. Moreover, the zeolite acidity may influence the catalytic and electronic properties of the active phase as was shown for metal catalysts [5] and by some of us for ruthenium sulfide [6]. In this previous study, we showed that the properties of nanoparticles of ruthenium sulfide dispersed in a series of Y zeolites varied widely according to the nature of the zeolite, HY, KY, and dealuminated HY_d and KHY_d. For the reactions of hydrogenation of tetralin and toluene carried out in the presence of H_2S the difference of activity was very high (difference of activity between the most and the least active catalyst circa 200 times for tetralin hydrogenation). This increase in activity for the hydrogenation of aromatics was related to the electron-deficient character of the sulfide particles in the acidic zeolites as it had been proposed for metal catalysts [7].

* Corresponding author.
E-mail address: breysse@ccr.jussieu.fr (M. Breysse).

0021-9517/$ – see front matter
doi:10.1016/S0021-9517(03)00308-7

The objective of the present study is to examine if such modifications of the electronic and catalytic properties also occur for molybdenum sulfide. As a matter of fact, most of the hydrotreatment catalysts are molybdenum sulfide-based catalysts. It is then most important to determine which parameters influence the hydrogenation properties of the catalyst, hydrogenation steps being involved in hydrodesulfurization and hydrodenitrogenation reactions schemes. Besides, the hydrogenation of aromatics is also an important issue.

For such a study, it is important to separate, as much as possible, the various parameters, which may influence the activity, i.e., the location of the active phase in the porosity, the number, and strength of the acid sites. The β-zeolite system has been preferred to the Y-zeolite system because it is possible to monitor the acidity by dealumination without noticeable loss of cristallinity and important formation of extraframework alumina owing to nitric acid treatments [8]. For Y zeolites, dealumination leads to the formation of highly disordered mesopores and the presence of strongly acidic extraframework alumina is difficult to avoid [9]. In the present study, we utilized a series of β-zeolites with acidic properties varying in a wide range, the initial β-zeolite with a Si/Al ratio equal to 13.8, two partially dealuminated samples (Si/Al = 15.0 and 18.7) and a fully dealuminated one (Si/Al > 800). In the nonacidic fully dealuminated zeolite, molybdenum was introduced by impregnation with ammonium heptamolybdate. In the acidic supports, molybdenum was introduced by cation exchange with $[Mo_3S_4(H_2O)_9]^{4+}$ as was proposed by Taniguchi et al. [10,11]. Ammonium heptamolybdate impregnation was also utilized for one of the acidic supports for comparison purposes. All the samples were sulfided in a stream of H_2/H_2S and characterized by HRTEM. The characteristics of the acidic and hydrogenating sites were studied by IR spectroscopy. On sulfided samples activated in situ, CO adsorption experiments were performed at 100 K in order to avoid any modification of the active phase by the probe molecule adsorption and to allow CO interaction with zeolite OH groups. The weak adsorption of CO on Brönsted acid sites can be used to determine the acidity of the protons. This probe molecule also provides information related to the electronic properties of the MoS_2 particles dispersed in the zeolite. The catalytic properties were determined in the hydrogenation of tetralin in the presence of H_2S. This model molecule was chosen because it is representative of the aromatics present in gas oils.

2. Experimental

2.1. Catalysts

The parent TEAHβ zeolite provided by RIPP (China) was calcined to obtain the acidic Hβ. Calcination was performed under air flow by increasing the temperature (1.5 K min^{-1}) up to 823 K and keeping the sample at this temperature for 4 h. The Si/Al ratio was 13.8. Dealumination was performed using the nitric acid treatment described in Refs. [8–12]. The amount of 2.5 g of zeolite was mixed with 250 mL of nitric acid solution of various concentrations ([HNO_3]: 1.5 and 5.3 mol L^{-1}) and heated under reflux and stirring for 4 h. The solid was then gathered by centrifugation and washed four times in distilled water (250 mL). It was then dried at 363 K overnight in air and calcined under air (20 mL s^{-1}) with a heating rate of 1.5 K min^{-1} up to 823 K and then maintained at this temperature for 8 h in order to eliminate the remaining template. The fully dealuminated zeolite was prepared using concentrated nitric acid (69.5 wt%). This treatment eliminated also the template. According to their Si/Al ratios, these zeolites are referred to as β13.8, β15.0, β18.7, and β800. X-ray diffraction studies showed that the structure of the β-zeolite did not lose significant cristallinity during dealumination since the intensities of the two main (101) and (302) peaks at $2\theta = 7.6$ and 22.5°, respectively, remain almost unchanged and there was no amorphous phase visible in the background of the diffractograms. The microporous volume determined from the nitrogen adsorption isotherms by the t-plot method between $P/P_0 = 0.1$ and 0.3 did not change for β13.8, β15.0, β18.7, i.e, 0.24 ± 0.1 cm^3 g^{-1}, but was lower for β800, i.e., 0.17 cm^3 g^{-1}. This indicates that some mesopores were formed during the treatment with concentrated nitric acid, probably by merging of some micropores, since the total porous volume (micro + meso) was identical, i.e., 0.24 cm^3 g^{-1} ($P/P_0 = 0.9$).

$[Mo_3S_4(H_2O)_9]^{4+}$ was introduced by cation exchange in the presence of ammonia in β13.8, β15.0, and β18.7 so as to reach about 4.7 wt% of Mo [12]. The preparation method of the complex was published by Shibahara et al. [13]. The amount of 2.5 g of zeolite was mixed with 125 mL of distilled water. On the other hand, 310 mg of the $Mo_3S_4Cl_4/NH_4Cl$ mixture was dissolved in 125 mL of distilled water. The $[Mo_3S_4]^{4+}$ solution was added drop by drop to the zeolite suspension. When the pH was lower than 3, a few milliliters of NH_3 (0.33%) was added to increase the pH to 7. Again, the $[Mo_3S_4]^{4+}$ solution was added drop by drop, and so on. The final pH was 3. The mixture was stirred for 3 h at 313 K. Then, the suspension was filtered, and the solid was washed with 125 mL of distilled water and centrifuged again. This washing procedure was repeated three times. The solid was then dried at 313 K under vacuum overnight. Finally, the sample was calcined under argon (flow rate 3.6 L h^{-1}) at 623 K for 3 h (heating rate 5 K min^{-1}). The samples are referred to as Mo/β13.8, Mo/β15.0, and Mo/β18.7.

Mo was introduced by impregnation with ammonium heptamolybdate $(NH_4)_6Mo_7O_{24} \cdot 4H_2O$ (AHM) in the fully dealuminated β800 since this support does not contain exchangeable sites. This sample is referred to as IMo/β800. For comparison of the two preparation methods, a sample (β13.8) containing acid sites was impregnated with ammonium heptamolybdate (IMo/β13.8). For β800 1.5 mL g^{-1}

Table 1
Chemical compositions of the catalysts determined by chemical analysis

Sample	Mo (wt%)	S (wt%)	S/Mo
Mo/β13.8	4.0	2.93	2.20
Mo/β15.0	3.95	2.80	2.13
Mo/β18.7	4.26	2.96	2.08
IMo/β13.8	5.24	2.32	1.33
IMo/β800	8.2	4.89	1.79

and for β13.8 1.1 mL g^{-1} of AHM aqueous solution were put into contact with the zeolites support for 3 h. The samples were dried in air at 363 K for 12 h and then calcined under a flow of industrial air (Air Liquide, 3.6 L h^{-1}) from RT to 723 K with a heating rate of 5 K min^{-1} and then left at 723 K for 3 h. The various samples were sulfided using gas flows of 15% of H_2S in H_2 at atmospheric pressure. The temperature of the reactor was gradually increased at a rate of 10 K min^{-1} up to 673 K and maintained at this temperature for 4 h. The catalyst was cooled to room temperature under the same sulfiding atmosphere and flushed with N_2 for 30 min. The chemical compositions of the catalysts are given in Table 1.

2.2. Transmission electron microscopy

The electron microscopy was performed on a JEOL 2010 TEM (200 kV; point to point resolution, 0.195 nm) equipped with a EDS Link-Isis detector. Freshly sulfided samples were ground under an inert atmosphere and were ultrasonically dispersed in ethanol. The suspension was collected on carbon-coated grids.

2.3. Infrared spectroscopy

Catalyst acidity was determined by IR spectroscopy using CO, as probe molecule. The FTIR spectra were recorded with a Magna spectrometer from Nicolet using 256 scans and a resolution of 4 cm^{-1}. About 12 mg of samples (precisely weighted) calcined as described above were pressed as self-supported wafers (diameter 1.6 cm). After introduction of the wafers into the IR cell, equipped with CaF_2 windows and presenting double walls with a space for cooling agent, the samples were sulfided at 673 K (ramp 10 K min^{-1}) under a flow of H_2/H_2S 15% for 4 h. Then, the samples were evacuated at 673 K at a residual pressure of 10^{-5} Torr. The samples were further cooled down to 100 K under vacuum. A first spectrum of the wafer was recorded as reference. Then, given amounts of CO were introduced and IR spectra were recorded for each dose. The spectra were normalized to an equivalent sample mass of 10 mg. The spectra of adsorbed CO reported in this study are in fact substracted spectra, i.e., the spectra of adsorbed CO minus the reference spectrum of the sample before CO adsorption.

2.4. Catalytic activity measurements

Experiments were carried out in a high-pressure microreactor system operated in the dynamic mode in the gas phase in the following conditions: $P_{tot} = 4.5$ MPa, $P_{tetralin} = 5.9$ kPa, $P_{H_2S} = 1.5$ kPa, 573 K. Tetralin was introduced in the reactor by means of a gas-phase saturator. After a first period of deactivation, all the catalysts deactivate very slowly and approximately at the same rate. Consequently, the conversions were measured after 18 h on stream. Reaction rates, V_s, specific rate (per gram of catalyst), and V_i, intrinsic rate (per Mo atom), were calculated according to the following relations.

$$V_s \ (\text{mol}\, g^{-1}\, s^{-1}) = -F\big(\ln(1-\tau)\big)m^{-1},$$

with F as molecular flow, τ as conversion, m as catalyst weight. $V_i \ (\text{mol at}_{Mo}^{-1}\, s^{-1}) = V_s M_{Mo} (\%Mo)^{-1}$, with M_{Mo} as Mo molecular weight, % Mo per gram of catalyst determined by chemical analysis.

Under these experimental conditions, tetralin is hydrogenated in *cis*- and *trans*-decalin or dehydrogenated in naphtalene. In the presence of acid catalysts, isomerization of one of the ring occurs leading to 1 or 2-methylindane or 1 or 2-methylperhydroindane. Then, the C5 cycle can be opened and cracked into light products.

3. Results

3.1. Electron microscopy

Fig. 1 shows some examples of electron micrographs of Mo/β13.8, Mo/β18.7, and IMo/β800 after the sulfidation treatment. All the micrographs of the acidic zeolites present the same features: small square particles of 200 to 800 nm of well-crystallized zeolite coated by a thin braid of molybdenum sulfide particles. It is difficult to visualize both the MoS_2 slabs and the zeolite structure under the same focus conditions. These structures can be clearly seen in Fig. 1A (MoS_2) and 1B (zeolite structure). At higher magnification, some tiny MoS_2 particles are also observed in the zeolite framework (Fig. 1B). These figures show that the structure of the zeolite is retained and no difference of size of the MoS_2 particles appears between the samples. EDX analysis was performed on the Mo/β13.8 sample and focused on the center of the particle. The average of 15 measurements of the Mo/Si ratio was found equal to 0.38, which is very close to the chemical analysis, i.e., 0.35. This indicates an homogeneous distribution of molybdenum in the zeolite. The same method gives for the S/Mo ratio an average value of 2.

For the impregnated sample IMo/β800, the micrographs are different, MoS_2 is distributed as particles of circa 4 nm in the zeolite (or on its surface) and some large particles of MoO_3 sulfided at the surface only appear as a separate phase (unpublished results). A quantification of the amount of Mo as MoS_2 inside the zeolite framework or at the surface was

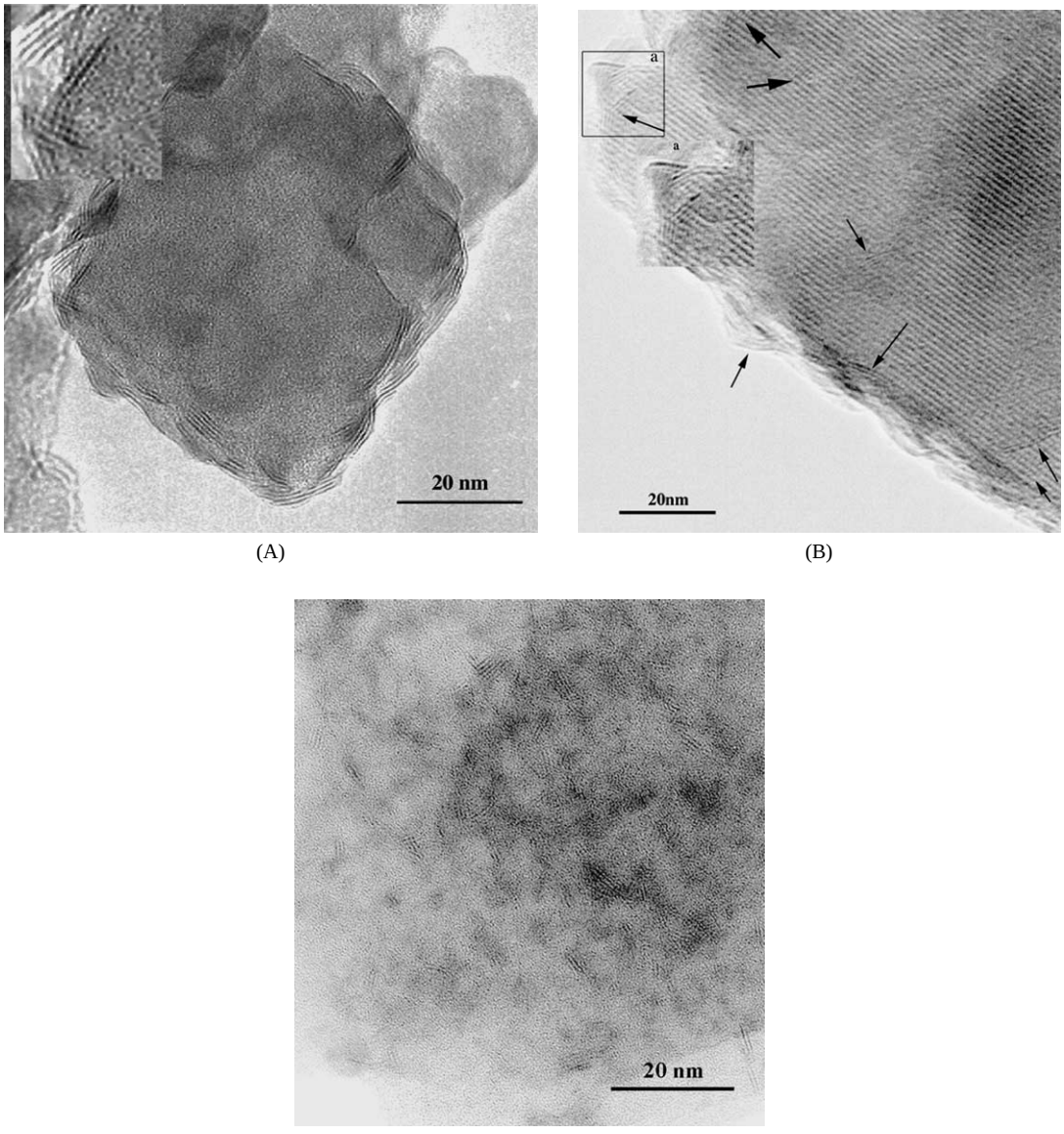

(A) (B)

(C)

Fig. 1. Electron micrographs of molybdenum sulfide supported on β-zeolites: (A) Mo/β13.8; (B) Mo/β18.7; (C) IMo/β800.

performed taking into account the results of 30 EDX analyses of various parts of the sample compared to chemical analysis. These measurements allow estimation that nearly 60% of Mo is present as MoS_2 particles well distributed in the zeolite grains and on the surface whereas 40% of Mo is present as MoO_3 particles coated by MoS_2. This biphasic character explains why the ratio S/Mo of the impregnated samples is lower than that of the samples prepared with the thiocomplex (Table 1).

3.2. Infrared spectroscopy

All the acidic β samples exhibit a ν_{OH} band at 3740 cm^{-1} characteristic of silanol groups, another band is detected at 3610 cm^{-1} characteristic of bridged AlOHSi of the zeolite framework (Fig. 2). The weak bands at 3780 and at

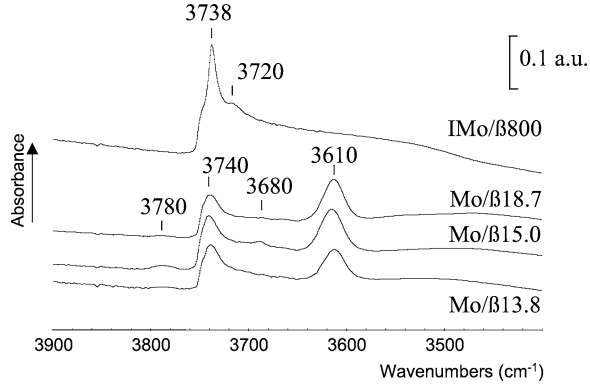

Fig. 2. IR spectra of ν(OH) vibration zone of the various sulfided Mo zeolites.

3680 cm^{-1} are ascribed to AlOH. The broad weak band appearing at a lower wavenumber (around 3470 cm^{-1}) should indicate some interaction between OH groups and Mo phase. The IR spectrum of the β800 sample in the ν_{OH} range (Fig. 2) is very close to that observed on pure silica [14]. It shows a sharp band at 3738 cm^{-1} characteristic of isolated silanol groups as well as a shoulder at 3720 cm^{-1} attributed to terminal silanol. The broad band around 3500 cm^{-1} should characterize silanol "nests" as deduced from Ref. [14]. It is noted that the bands at 3780, 3680, and 3610 cm^{-1} are absent in this sample as expected because of aluminum removal.

3.2.1. Adsorption of CO on the Mo/β15.0 sample

When the first small dose of CO is introduced at 100 K on Mo/β15.0, the OH bands are not perturbed (Fig. 3A). The addition of increasing amounts of CO leads to an interaction with the OH groups since their frequencies are shifted toward lower wavenumbers (Fig. 3A). The larger these wavenumber shifts, the more acidic the hydroxyl groups. As observed in Fig. 3A, CO interacts first with the zeolite OH groups at 3610 cm^{-1} and shifts this band down to 3280 cm^{-1}. Taking into account the shift of the OH band, 330 cm^{-1}, we can conclude that the Brönsted acidity is very strong [15,16]. The number of perturbed zeolitic OH groups increases with the amount of CO, and then CO begins to interact with silanol groups. In this case, the extent of the perturbation is weaker since the OH band shifts from 3740 to 3640 cm^{-1}.

In the ν(CO)-stretching zone, the introduction of small doses of CO gives rise to a weak band at 2143 cm^{-1} (Fig. 3B). Its presence is not related to a perturbation of ν(OH) bands but ascribed to CO in interaction with the molybdenum sulfide phase. For further doses of CO, a ν(CO) band appears at 2178 cm^{-1}, which progressively shifts to 2175 cm^{-1}. This shift can be related to site heterogeneities, the strongest sites being saturated first. The intensity of this band increases in parallel with the perturbation of the OH band at 3610 cm^{-1}. This allows us to attribute this band to CO in interaction with the strong acidic zeolitic OH groups. A weak band at 2189 cm^{-1} is also detected, whose intensity is quickly saturated with further CO doses. It characterizes CO coordinated to Al^{3+}. Above 6.6 µmol of CO, a ν(CO) band at 2159 cm^{-1} is detected when the perturbation of the silanol band is observed. This wavenumber is in agreement with previous studies on silica [15]. The weaker acidity of the silanol groups is consistent with the fact that the ν(CO) band at 2159 cm^{-1} only appears at high CO pressure. For the highest doses, a band and shoulder at 2143 and 2134 cm^{-1} attributed to CO physisorbed on the zeolite are observed.

3.2.2. Comparison of the zeolite acidities

CO adsorption on the other acidic β-zeolites gives rise to similar features. Nevertheless, it appears that the intensity of the band at 2175 cm^{-1} increases with the alumina content of the zeolite framework (Fig. 4A). By contrast, the spectrum of IMo/β800 does not present any bands at 2175 and 2189 cm^{-1}. This is consistent with the fact that there is almost no aluminum in this zeolite. Only the band at 2159 cm^{-1} corresponding to CO interacting with silanol groups is observed for this sample. The bands attributed to CO physisorbed are present for all the samples. In order to get quantitative information concerning the amount of strong Brönsted acid sites in the samples, the spectra corresponding to the highest CO dose introduced were decomposed into 5 bands, and the surface area of the corresponding band at 2175 cm^{-1} was measured. Fig. 4B shows that the number of strong acid sites determined by this method is proportional to the calculated number of H^+ per unit cell.

3.2.3. Adsorption on the molybdenum sulfide phase

As already noted above, when weak amounts of CO (0.1 to 1.6 µmol) are introduced on the Mo/β15 sample, a ν(CO) band can be distinguished at 2143 cm^{-1} characteristic of the molybdenum sulfided phase (Fig. 3B). For the other samples (Fig. 5A), an equivalent low wavenumber band is detected at 2158 cm^{-1} for Mo/β13.8, at 2133 cm^{-1} for Mo/β18.7,

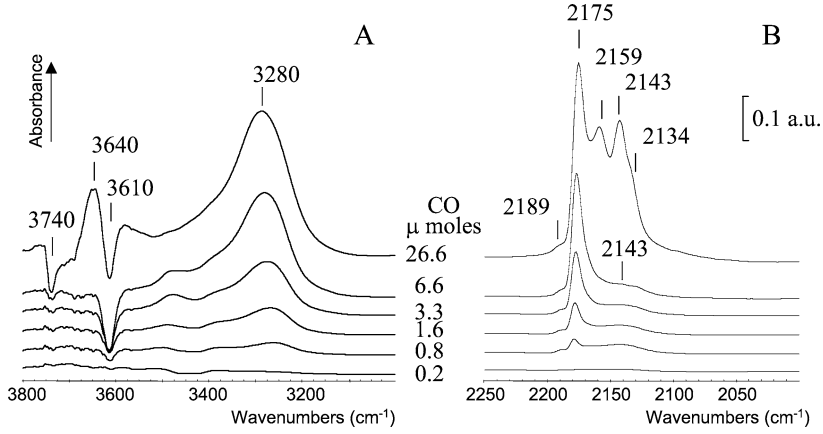

Fig. 3. IR spectra of CO adsorbed (small calibrated doses, $T_{ads} = 100$ K) on sulfided Mo/β15.0: (A) in the OH vibration range; (B) in the CO vibration range.

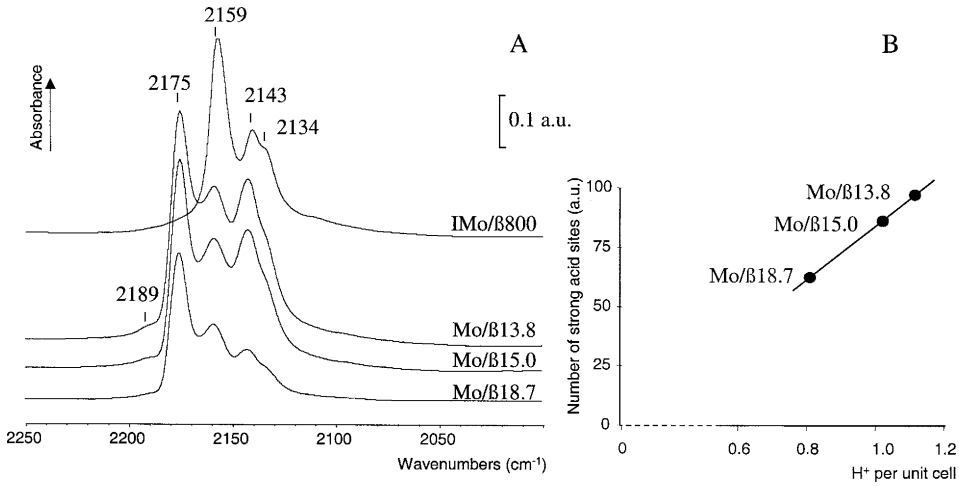

Fig. 4. (A) IR spectra of CO adsorbed (26.6 µmol, $T_{ads} = 100$ K) on the various sulfided Mo zeolites; (B) number of strong acid sites in Mo/β versus the number of H^+ per unit cell.

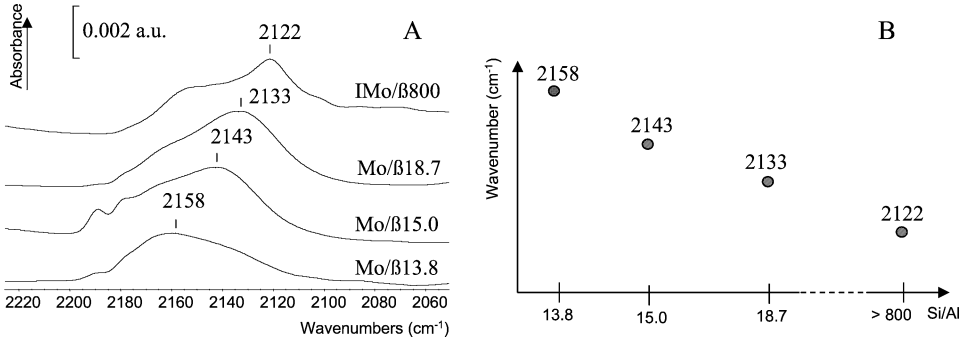

Fig. 5. (A) IR spectra of CO adsorbed (0.4 µmol, $T_{ads} = 100$ K) on the various sulfided Mo zeolites; (B) variation of ν(CO) wavenumber of CO adsorbed on molybdenum sulfide dispersed in the β-zeolites of various acidities.

and at 2122 cm^{-1} on IMo/β800 (in agreement with independent results obtained on reference silica). The position of these bands is very close to those of physisorbed CO. However, two factors prevent their attribution to physisorbed CO species: (i) they are saturated for such low CO amount, and (ii) they remain after an evacuation at low temperature. Moreover, several shoulders (at 2188, 2177, and 2158 cm^{-1}) are observed on Fig. 5A. Their wavenumbers coincide with the frequencies of CO bands on the zeolites and their intensities continuously increase when supplementary CO doses are added. This discards their attributions to CO adsorbed on sulfided particles.

The position of the main band corresponding to CO in interaction with the MoS_2 phase increases with the zeolite acidity (Fig. 5B). Studies performed with other supports confirm this trend [17]. In addition, Fig. 5A shows that the bands characteristic of CO in interaction with the Mo particles are very weak and are saturated at very low amounts of CO. This reveals that the dispersion of the MoS_2 particles is low. Taking into account the amount of CO necessary to saturate these sites, we could estimate a dispersion equivalent to that measured for a MoS_2 catalyst supported on silica (7% Mo deposited by dry impregnation) for our four samples.

3.3. Catalytic activities

3.3.1. Comparison of the results obtained by the two preparation methods for Mo/β13.8

IMo/β13.8 prepared by heptamolybdate impregnation is less active than Mo/β13.8 obtained from the thiocomplex (19.0 and 31.8 10^{-4} mol at_{Mo}^{-1} s^{-1}, respectively (Fig. 6)). This lower activity might be related to the biphasic character of this sample, which contains only 60% of the molybdenum as well as dispersed molybdenum sulfide entities (Section 2.1) by contrast to the thiocomplex preparation, which only leads to molybdenum sulfide.

3.3.2. Influence of the Si/Al ratios

The catalytic properties of the various samples vary in a wide range (Fig. 6), the total conversion of the most acidic sample being 100 times higher than that of the nonacidic IMo/β800. However, for the most acidic samples, isomerization and cracking reactions represent a large part of the conversion. If we consider only the hydrogenation and dehydrogenation properties, the activity of Moβ/13.8 is circa 40 times higher than that of Moβ/800, the properties of Mo/β15.0 and Moβ/18.7 being intermediate (Table 2). Moreover, parallel variations of the catalysts acidities,

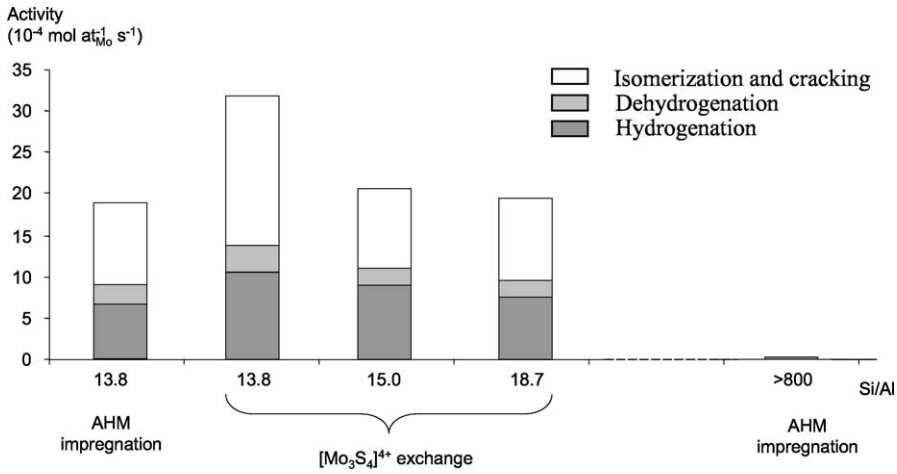

Fig. 6. Catalytic properties in tetralin hydrogenation of the Mo/β catalysts; $T = 573$ K, $P_{tot} = 4.5$ MPa, $P_{H_2S} = 1.5$ kPa.

Table 2
Number of acid sites measured by IR and catalytic properties

Mo/β samples	Number of acid sites measured by IR (a.u.)	Hydrogenation–dehydrogenation activities (10^{-4} mol at_{Mo}^{-1} s^{-1})
Mo/β13.8	100	13.7
Mo/β15.0	88	11
Mo/β18.7	65	9.5
Mo/β800	0	0.3

measured by IR spectroscopy, and of the hydrogenation–dehydrogenation properties are observed.

4. Discussion

4.1. Dispersion and location of the molybdenum sulfide phase

Using the conventional method of impregnation by heptamolybdate impregnation, part of the molybdenum was not introduced in the zeolite porosity and was present as MoO_3 coated by a layer of MoS_2. This explains why the ratio S/Mo for the IMo/β800 sample and IMo/β13.8 was lower than 2 (Table 1). This means that part of the molybdenum was not active for the hydrogenation of tetralin. In order to overcome this difficulty, we utilized a thiocomplex and introduced it by ion exchange in the presence of ammonia in the acidic zeolites. This method avoids the formation of particles of MoO_3, and the values of the S/Mo ratios close to 2, determined by chemical analysis (Table 1), indicate that MoS_2 entities were formed. This result is confirmed by EDX since a value of S/Mo close to 2 has been also found for Mo/β13.8. However, the dispersion of MoS_2 in the acidic zeolites is not as uniform as we could have expected since some MoS_2 is clearly located on the external surface of the zeolite particles and some small entities inside the particles. The presence of MoS_2 on the zeolite particles may arise either from the migration of the molydenum sulfide precursor toward the external surface of the zeolite particles in the presence of physisorbed water in the zeolite cages as was proposed by de Bont et al. [18], or from the polymerization of the thiocomplex during the preparation, which would lead to an enrichment in MoS_2 at the surface of the particle. However, with zeolite of strong Brönsted acidity, the local pH both in the structural pores and on the external surface of the particles can be expected to be much lower than in solution. Therefore, the hypothesis of a depolymerization allowing cationic exchange cannot be ruled out. This would explain the presence of small MoS_2 particles inside the porosity. In any case, this phenomenon is observed for the whole series of acidic samples. The fact that the catalytic activities vary within a large range (a factor of 40) with acidity, suggests that a part of MoS_2 is inside the porosity. Other factors, such as acidity modifying the morphology of the MoS_2 particles are probably not involved as suggested by our previous work on RuS_2 [6]. As a matter of fact, no variation of the morphology of the RuS_2 particles was observed for a series of Y zeolites of different acidities while catalytic activities varied in a wide range.

4.2. Electronic properties of the molybdenum sulfide phase and relation to catalytic properties

The properties of metal particles dispersed in acidic or basic zeolites were studied by many authors. Already in 1973, Figueras et al. [19] found that the activities of PdY zeolites for benzene hydrogenation were enhanced when Brönsted acid sites or multivalent cations were present. Later on, the enhancement of the catalytic properties of metal particles, dispersed on acidic supports compared to neutral supports, for hydrogenation reactions, hydrogenolysis reactions, and isomerization reaction was observed by many authors [5,20,21]. In parallel, it was found that the activity of Pt in basic zeolites decreased when the basicity of the support increased [22,23]. The term “electron deficiency” was first introduced by Dalla Batta and Boudart [7] to account for these variations in the properties of the Pt particles. The electron deficiency was ascribed to an electron transfer

from small Pt particles to the zeolite and evidenced experimentally by X-ray absorption and FTIR studies of adsorbed CO [24]. Recently, Koningsberger and co-workers [25] measured the catalytic properties of Pt catalysts for several reactions, neopentane hydrogenolysis and tetralin hydrogenation in the presence of 165 parts per million weight dibenzothiophene added to the feed. They found that for all these reactions, the TOF increased with increasing acidity. The nature of the metal–support interaction in supported Pt catalysts was determined by spectroscopic atomic XAFS (AXAFS) and theoretical calculation. These studies reveal that the nature of the metal–support interaction involves a change in the electronic properties of the metal cluster, induced by and correlated to the electron richness of the support oxygen atom. In a more recent work, this group has shown that the support basicity determines the Pt–H bond strength and this ultimately causes a change in coverage and bond strength of both the H and the alkane [26].

By comparison to the numerous studies concerning metals, the influence of the support acidity on the properties of sulfide catalysts is much less documented, although NiMo sulfide is often associated with a HY zeolite in the composition of hydrocracking catalysts. It was noted in studies related to hydrodesulfurization that the presence of acid sites increased the properties of the sulfide phase. For Vissenberg et al. [27], this effect cannot be explained only by an improvement of dispersion. Possibly, the protons themselves play an active role in the HDS reaction or act as a structural promoter by increasing the electron-deficient character of the metal sulfide.

As noted in the Introduction, some of us studied the properties of ruthenium catalysts dispersed in a series of Y zeolites with various acidic properties [6]. The wavenumbers of the ν(CO) bands of Ru metal particles varied between 2051 cm^{-1} for the nonacidic KY support and 2063 cm^{-1} for the acidic HY zeolites dealuminated or not. As a consequence, the stronger the acidity of the zeolite, the higher the ν(CO) frequency characterizing the Ru sites. In parallel, the ν(CO) wavenumbers of the ruthenium sulfide particles dispersed in the same supports varied from 2056 cm^{-1} (KY zeolite) to 2071 cm^{-1} (HY zeolites). In both cases, metal and sulfide, we interpreted the modifications of the ν(CO) wavenumber in terms of electronic transfer between the zeolite and the active phase particles. The very high variation (circa 200) of the catalytic activity in aromatics hydrogenation of the ruthenium sulfide clusters was ascribed to the modification of their electronic properties, the dispersion of the sulfide active phase and its stoichiometry being not affected by the presence of acid sites. A superimposed influence of the acidic sites on the adsorption of the aromatic molecules was not excluded.

In the present study, the ν(CO) wavenumber characterizing the adsorption of CO on the molybdenum sulfide phase increases regularly from 2122 cm^{-1} for the nonacidic sample to 2158 cm^{-1} for the most acidic one. In agreement with the studies related to ruthenium sulfide, we ascribed these variation to an electron transfer between the sulfide particles and the zeolites. The stronger the acidity, the higher the ν(CO) frequency characterizing the molybdenum sulfide sites. It should be noted that this is the first observation of a regular variation of the ν(CO) wavenumber within a series of supports of various acidities, although FTIR studies of CO adsorption had already been used for characterizing the properties of molybdenum sulfide, either supported on alumina [28] or unsupported [29]. In the same way, an increase of the ν(CO) value has also been recently observed on unpromoted and promoted sulfide tungsten phase supported on amorphous silico-alumina supports with various amounts of acidic OH groups [30].

As a consequence of these variations of the electronic properties of the active phase, a modification of the catalytic properties is expected. As a matter of fact, the hydrogenating properties of the catalysts of the present study vary regularly and in a wide range with the supports acidity. It must be noted that the very low activity of IMo/β800 is not due to the different preparation method, since the catalytic activity of IMo/β13.8 is only twice lower than that of Mo/β13.8.

With the data presented here, we cannot discuss further the sulfide–support interaction; particularly, we cannot address the consequence of these variations on the adsorption of the reactant, tetralin or hydrogen. This would require further delicate kinetic and physico-chemical studies. However, the impact of the present results on the design of more active catalysts is obvious since hydrogenation steps are involved in all hydrotreating reactions. Further results in hydrodesulfurization will be published in the near future.

5. Conclusion

The results presented in this paper show that the Brönsted acidity of the zeolite used to disperse molybdenum sulfide has a marked influence on the catalytic and electronic properties of the active phase. This means that the concept of changing the properties of metal particles by changing the acid/base properties of the support can be extended to transition metal sulfide support interaction. This finding may have important practical consequences on the design of more active catalysts for various hydrotreating reactions providing that acidity can be tuned to avoid undesirable side reactions. Further studies must be carried out in this direction using less acidic supports such as as MCM or SBA materials.

Acknowledgments

This work was carried out within the framework of a contract entitled Hydrodésulfuration Poussée des Gazoles. It was supported by CNRS, CNRS-ECODEV, ELF, IFP, Procatalyse, and TOTAL. Special thanks to Slavik Kasztelan for his interest and support on this subject. The authors are grateful to Mrs. Martine Cattenot, Mrs. Bernadette Jouguet,

and Mrs. Marie-Dominique Appay for their help in catalytic activity measurements and HRTEM experiments. M.B. also thanks Prof. Koningsberger for interesting discussions.

References

[1] H. Topsøe, B.S. Clausen, F.E. Massoth, in: J.R. Anderson, M. Boudart (Eds.), Catalysis, Science and Technology, Vol. 11, Springer, Berlin, Heidelberg, 1996.
[2] D.D. Whitehurst, T. Isoda, I. Mochida, Adv. Catal. 42 (1998) 345.
[3] M. Breysse, J.-L. Portefaix, M. Vrinat, Catal. Today 10 (1991) 489.
[4] P. Michaud, J.-L. Lemberton, G. Pérot, Appl. Catal. A 169 (1998) 343.
[5] P. Gallezot, Catal. Rev.-Sci. Eng. 20 (1979) 121.
[6] M. Breysse, M. Cattenot, V. Kougionas, J.-C. Lavalley, F. Mauge, J.-L. Portefaix, J.-L. Zotin, J. Catal. 168 (1997) 143.
[7] R.A. Dalla Batta, M. Boudart, in: J.H. Hightower (Ed.), Proc. Intern. Congr. Catal., Miami, 1973, p. 1329.
[8] E. Bourgeat-Lami, F. Fajula, D.A. Anglerot, T. des Courières, Micropor. Mater. 1 (1993) 237.
[9] C. Sun, M.-J. Peltre, M. Briend, J. Blanchard, K. Kajerwerg, J.-M. Krafft, M. Breysse, M. Cattenot, M. Lacroix, Appl. Catal. A, in press.
[10] M. Taniguchi, Y. Ishii, T. Murata, M. Hidai, T. Tatsumi, Stud. Surf. Sci. Catal. 105 (1997) 893.
[11] M. Taniguchi, D. Imamura, H. Ishige, Y. Ishii, T. Murata, M. Hidai, T. Tatsumi, J. Catal. 187 (1999) 139.
[12] C.-E. Hédoire, E. Cadot, C. Louis, A. Davidson, M. Breysse, submitted for publication.
[13] T. Shibahara, M. Yamasaki, G. Sukane, K. Minami, T. Yabuki, A. Ichimura, Inorg. Chem. 31 (1992) 640 .
[14] A. Burneau, J.P. Gallas, in: Vibrational spectroscopies, The Surface Properties of Silica, Wiley, New York, 1998.
[15] T. Chevreau, J.-C. Lavalley, J. Chem. Soc., Faraday Trans. 94 (1998) 3039.
[16] A. Janin, M. Maache, J.-C. Lavalley, J.F. Joly, E. Benazzi, Zeolite 11 (1991) 391.
[17] G. Crepeau, PhD thesis, Caen, 2002.
[18] P.W. de Bont, M.J. Vissenberg, V.J.H. de Beer, J.A.R. van Veen, R.A. van Santen, A.M. van der Kraan, Appl. Catal. A 202 (2000) 99.
[19] F. Figueras, R. Gomez, M. Primet, Adv. Chem. Ser. 121 (1973) 480.
[20] S.D. Lin, M.A. Vannice, J. Catal. 14 (1993) 539.
[21] M. Vaarkamp, J.T. Miller, F.S. Modica, G.S. Lane, D.C. Koningsberger, in: Proceedings, 10th Intern. Congr. Catal., Budapest, 1992, p. 809.
[22] A. de Mallman, D. Barthomeuf, J. Chim. Phys. 87 (1990) 535.
[23] D. Barthomeuf, Catal. Rev.-Sci. Eng. 38 (1996) 521.
[24] T.M. Tri, J.P. Candy, P. Gallezot, J. Massardier, M. Primet, J.C. Védrine, B. Imelik, J. Catal. 79 (1983) 396.
[25] D.E. Ramaker, J. de Graaf, J.A.R. van Veen, D.C. Koningsberger, J. Catal. 203 (2001) 7.
[26] D.C. Koningsberger, M.K. Oudenhuijzen, J. de Graaf, J.A. van Bokhoven, D.E. Ramaker, J. Catal., in press.
[27] M.J. Vissenberg, P.W. de Bont, W. Gruitjers, V.J.H. de Beer, A.M. van der Kraan, R.A. van Santen, J.A.R. van Veen, J. Catal. 189 (2000) 209.
[28] A. Travert, C. Dujardin, F. Maugé, S. Cristol, J.F. Paul, E. Payen, D. Bougeard, Catal. Today 70 (2001) 255.
[29] F. Maugé, J. Lamotte, N. Nesterenko, O. Manoilova, A.A. Tsyganenko, Catal. Today 70 (2001) 271.
[30] F. Maugé, G. Crépeau, A. Travert, T. Cseri, ACS Preprint, Division of Petroleum Chemistry, 2003, in press.